Relative flow fluctuations as a probe of initial state fluctuations

Giuliano Giacalone,[1] Jacquelyn Noronha-Hostler,[2] and Jean-Yves Ollitrault[1]

[1] *Institut de physique théorique, Université Paris Saclay, CNRS, CEA, F-91191 Gif-sur-Yvette, France*
[2] *Department of Physics, University of Houston, Houston TX 77204, USA*

(Dated: February 7, 2017)

Elliptic flow, v_2, and triangular flow, v_3, are to a good approximation linearly proportional to the corresponding spatial anisotropies of the initial density profile, ε_2 and ε_3. Using event-by-event hydrodynamic simulations, we point out when deviations from this linear scaling are to be expected. When these deviations are negligible, relative v_n fluctuations are equal to relative ε_n fluctuations, and one can directly probe models of initial conditions using ratios of cumulants, for instance $v_n\{4\}/v_n\{2\}$. We argue that existing models of initial conditions tend to overestimate flow fluctuations in central Pb+Pb collisions, and to underestimate them in peripheral collisions. We make predictions for $v_3\{6\}$ in noncentral Pb+Pb collisions, and for $v_3\{4\}$ and $v_3\{6\}$ in high-multiplicity p+Pb collisions.

I. INTRODUCTION

Anisotropic flow is the key observable providing evidence for the creation of a collective medium in ultra-relativistic heavy-ion collisions. In the current paradigm of bulk particle production [1], anisotropic flow emerges from the hydrodynamical response of the created medium to the anisotropies of its initial energy density profile [2]. Hydrodynamic simulations [3–5] show that elliptic flow, v_2, and triangular flow, v_3, correlate almost linearly with the initial eccentricity, ε_2, and triangularity, ε_3, respectively, of the system. Since the initial energy density profile is shaped out of stochastic nucleon-nucleon interactions, both initial anisotropies and flow coefficients fluctuate on a event-by-event basis [6]. To the extent that v_n is proportional to ε_n, the probability distribution of v_n [7] coincides, up to a global rescaling, with the probability distribution of ε_n [8, 9]. The latter is provided by models of initial conditions.

Many models of initial conditions have been proposed for proton-nucleus and nucleus-nucleus collisions. Some are based on variations of the Monte-Carlo Glauber model [10–14], others are more directly inspired from high-energy QCD, and involve, in particular, the idea of gluon saturation [15–20]. Initial anisotropies probe the geometrical shape of the initial density profile, and, thus, provide an information which is independent of the multiplicity distribution, which is the typical observable to which models are tuned. By determining which models are compatible with anisotropic flow data, one, therefore, expects to obtain new insight into the early dynamics of the collision.

In this paper, we analyze the relative fluctuations of v_2 and v_3 in p+Pb and Pb+Pb collisions at LHC energies. The observables we choose for this analysis are ratios of cumulants of the distribution of v_n, whose definition is recalled in Sec. II. In Sec. III, we compute the lowest non-trivial cumulant ratios $v_2\{4\}/v_2\{2\}$ and $v_3\{4\}/v_3\{2\}$ in event-by-event hydrodynamic simulations of Pb+Pb collisions and determine in which centrality intervals they are compatible with the corresponding ratios for ε_n. In these centrality intervals, we use existing experimental data to test the validity of initial condition models. We then make predictions for the ratio $v_3\{6\}/v_3\{4\}$. This study is carried over to p+Pb collisions in Sec. IV, where we make predictions for $v_3\{4\}/v_3\{2\}$ and $v_3\{6\}/v_3\{4\}$,

II. CUMULANTS AND RELATIVE FLUCTUATIONS

Anisotropic flow is the observation of a full spectrum of nonzero Fourier coefficients characterizing the azimuthal distribution of final-state particles in heavy-ion collisions. Denoting the final-state azimuthal distribution by $P(\phi)$, its Fourier decomposition reads

$$P(\phi) = \frac{1}{2\pi} \sum_{n=-\infty}^{+\infty} V_n \mathrm{e}^{-in\phi}, \tag{1}$$

and the quantity $v_n \equiv |V_n|$ is the coefficient of anisotropic flow in the nth harmonic. In experiments, the number of final-state particles is not large enough to allow the computation of the Fourier series of Eq. (1) in every event. Flow coefficients are computed from azimuthal multi-particle correlations, which are averaged over many events. Since $P(\phi)$ is different in each collision, anisotropic flow coefficients fluctuate on a event-by-event basis. Detailed information about the probability distribution of v_n can be obtained by measuring its cumulants. The cumulant of order m involves m-particle correlations as well as lower order correlations [21–23]: It is constructed by subtracting trivial contributions from lower-order correlations order by order. Cumulants are therefore considered the best signature of the collective origin of anisotropic flow in heavy-ion collisions. Nonzero values of higher-order cumulants have been measured in a wide range of collision systems, from Pb+Pb to p+p collisions [24–26].

The cumulants of the distribution of v_n are combinations of moments. Explicit expressions up to order eight

are [27]:

$$
\begin{aligned}
v_n\{2\}^2 &= \langle v_n^2 \rangle, \\
v_n\{4\}^4 &= 2\langle v_n^2 \rangle^2 - \langle v_n^4 \rangle, \\
v_n\{6\}^6 &= \frac{1}{4}\Big[\langle v_n^6 \rangle - 9\langle v_n^2 \rangle \langle v_n^4 \rangle + 12\langle v_n^2 \rangle^3\Big], \\
v_n\{8\}^8 &= \frac{1}{33}\Big[144\langle v_n^2 \rangle^4 - 144\langle v_n^2 \rangle^2 \langle v_n^4 \rangle + 18\langle v_n^4 \rangle^2 \\
&\qquad + 16\langle v_n^2 \rangle \langle v_n^6 \rangle - \langle v_n^8 \rangle\Big],
\end{aligned} \tag{2}
$$

where angular brackets denote an average over collision events in a given centrality class. Cumulants are defined in such a way that $v_n\{2k\} = v_n$ if v_n is the same for all events.

Any quantity which is linearly proportional to v_n has the same cumulants as v_n, up to a global factor. If the scaling between v_n and ε_n were exactly linear, then, for any even integers μ and ν [28],

$$
\frac{v_n\{\mu\}}{v_n\{\nu\}} = \frac{\varepsilon_n\{\mu\}}{\varepsilon_n\{\nu\}}. \tag{3}
$$

Ratios of cumulants quantify the relative fluctuations of v_n, which are equal to the relative fluctuations of ε_n if the scaling is linear [8, 29]. In particular, we use the first ratio $v_n\{4\}/v_n\{2\}$ as a measure of the relative fluctuations of v_n. The smaller the ratio, the larger the fluctuations. Higher-order ratios, such as $v_n\{6\}/v_n\{4\}$, probe the non-Gaussianity of the fluctuations [27, 30].

Ratios of cumulants are interesting because they are independent of the hydrodynamic response (the proportionality coefficient between ε_n and v_n), which is an important source of uncertainty when trying to constrain models of initial conditions from experimental data [31]. Eq. (3) directly relates experimental data (left-hand side) to models of initial conditions (right-hand side).[1] The approximate linearity of the relation between v_n and ε_n in event-by-event hydrodynamics is typically measured using scatter plots [4] or the Pearson correlation coefficient [3]. These approaches do not give any direct information on cumulant ratios, and on the accuracy of Eq. (3). In the next section, we test this equation directly through hydrodynamic calculations.

III. PB+PB COLLISIONS

We first test the validity of Eq. (3) for $v_2\{4\}/v_2\{2\}$ and $v_3\{4\}/v_3\{2\}$ by computing both sides of the equation in event-by-event hydrodynamics. We run hydrodynamic simulations of Pb+Pb collisions at $\sqrt{s} = 2.76$ TeV. The initial conditions from which initial anisotropies are computed are given by a Glauber Monte Carlo model [12, 32]. Initial density profiles are evolved by means of the viscous relativistic hydrodynamical code V-USPHYDRO [33–35]. We implement a shear viscosity over entropy ratio of $\eta/s = 0.08$ [36], and we compute flow coefficients at freeze-out [37] for pions in the transverse momentum range $0.2 < p_t < 3$ GeV/c. We compute $v_2\{4\}/v_2\{2\}$ and $v_3\{4\}/v_3\{2\}$ as function of centrality percentile. Between 1000 and 5000 events are simulated in each centrality window, each event corresponding to a different initial geometry. Results are shown in Fig. 1, and compared to the measurements of the ATLAS Collaboration [24]. A first remark is that $v_3\{4\}/v_3\{2\}$ is smaller than $v_2\{4\}/v_2\{2\}$. This means that v_3 fluctuations are larger than v_2 fluctuations, as expected since v_3 is solely due to fluctuations [38]. The smallness of $v_3\{4\}$ explains the large sta-

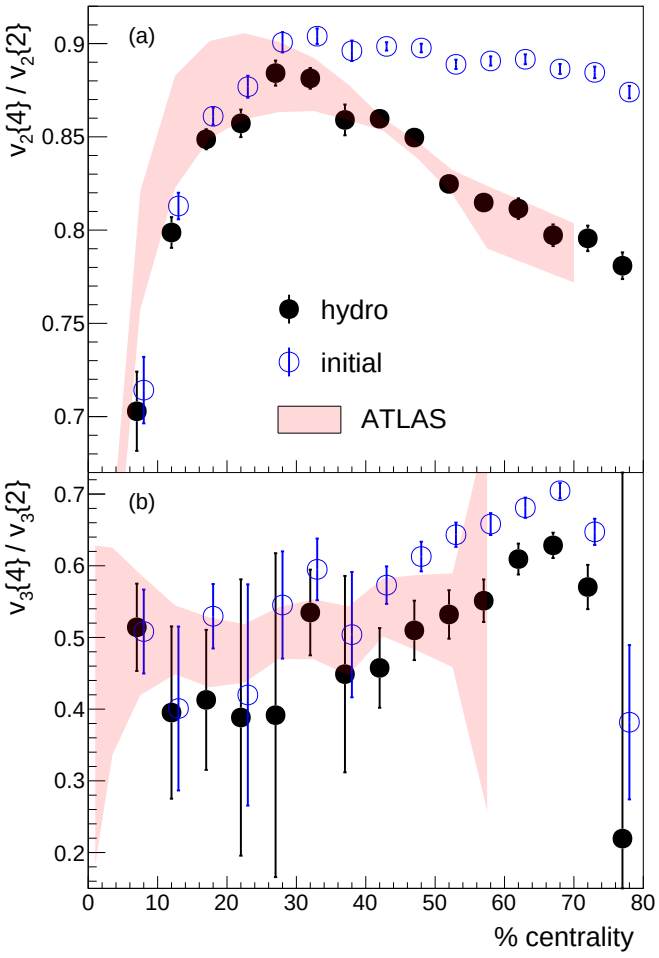

FIG. 1. (color online) Comparison between $v_n\{4\}/v_n\{2\}$ computed in hydrodynamics (full symbols), and $\varepsilon_n\{4\}/\varepsilon_n\{2\}$ computed from the corresponding initial energy density profiles (open symbols), for 2.76 TeV Pb+Pb collisions. Shaded bands: ATLAS data for $v_n\{4\}/v_n\{2\}$ [24]. Symbols are shifted horizontally for readability. (a) Elliptic flow ($n = 2$). (b) Triangular flow ($n = 3$).

[1] A similar analysis was recently carried out at RHIC energies within the AMPT model [28]

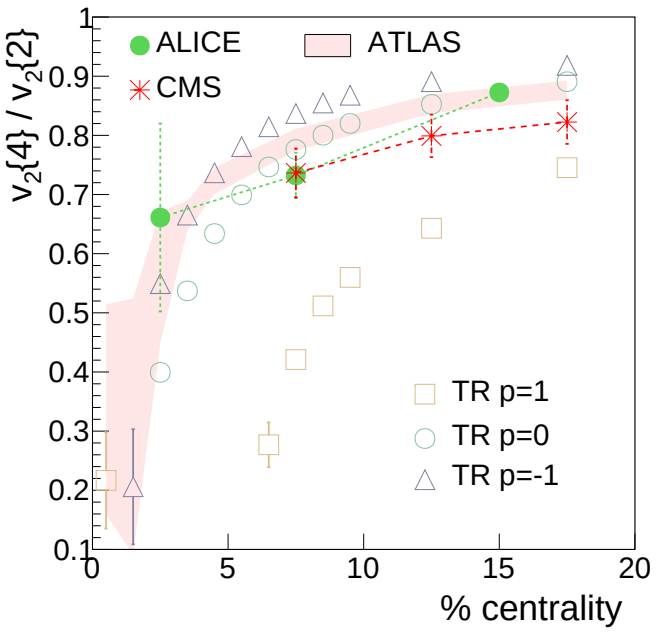

FIG. 2. (color online) Test of initial condition models using $v_2\{4\}/v_2\{4\}$ measured in Pb+Pb collisions at 2.76 TeV up to 20% centrality. Stars: CMS data [40]. Full circles: ALICE data [41]. Shaded band: ATLAS data [7]. Open symbols: values of $\varepsilon_2\{4\}/\varepsilon_2\{2\}$ given by the TRENTo model with $p = -1$ (triangles), $p = 0$ (circles) and $p = 1$ (squares).

tistical error on the corresponding ratio. We now discuss in turn $v_2\{4\}/v_2\{2\}$ and $v_3\{4\}/v_3\{2\}$. In centrality intervals where Eq. (3) is a good approximation, we test initial condition models against experimental data.

A. Elliptic flow fluctuations

We start with v_2 (Fig. 1 (a)). Eq. (3) holds approximately up to 20-30% centrality and gradually breaks down as the centrality percentile incraeses. The difference between $\varepsilon_2\{4\}/\varepsilon_2\{2\}$ and $v_2\{4\}/v_2\{2\}$ can be attributed to a cubic response term, proportional to $(\varepsilon_2)^3$ [39]. Once this nonlinear hydrodynamic response is taken into account, agreement with ATLAS data is excellent all the way up to 70% centrality. As we shall explain below, a similar nonlinear hydrodynamic response is also needed for other models of initial conditions in order to match experimental data.

Between 0 and 20% centrality, Eq. (3) holds to a good approximation. Therefore, in this centrality window, the ratio $\varepsilon_2\{4\}/\varepsilon_2\{2\}$ provided by initial condition models can be tested directly against experimental data for $v_2\{4\}/v_2\{2\}$. We test the sensitivity of this observable to initial conditions using TRENTo [42], a flexible parametric Monte Carlo model which effectively encompasses most of existing initial condition models [43]. The initial entropy density in TRENTo is expressed in terms of thickness functions, T_A and T_B, associated with each of the colliding nuclei. Each thickness function is a sum of Gaussians, centered around the participant nucleons. The weight of each participant nucleon is a random variable, so that the contribution of a participant to the deposited energy density may fluctuate. The strength of these fluctuations is regulated by a parameter, k (see Appendix A for details). Another parameter is the width of the Gaussians, σ. The initial density profile is assumed to be a homogeneous function of degree 1 of the thickness functions T_A and T_B, and a third parameter p specifies this dependence. The values $p = 1$, $p = 0$ and $p = -1$ correspond respectively to an arithmetic mean, $(T_A+T_B)/2$, a geometric mean, $\sqrt{T_A T_B}$, and a harmonic mean, $T_A T_B/(T_A + T_B)$. The case $p = 1$ correspond to the simple Glauber model where the density is proportional to the number of wounded nucleons [10]. The case $p = 0$ gives results close to QCD-inspired models such as IP-Glasma [18, 42] and EKRT [20, 43], while $p = -1$ is closer to the MC-KLN model [15, 43].

We have checked that $\varepsilon_2\{4\}/\varepsilon_2\{2\}$ and $\varepsilon_3\{4\}/\varepsilon_3\{2\}$ in Pb+Pb collisions depend little on the parameters k and σ. Therefore, we fix these parameters to the values suggested by the authors of Trento [42], which allow for a good description of the multiplicity distributions [14, 42]. On the other hand, cumulant ratios strongly depend on the third parameter, p. Results for $\varepsilon_2\{4\}/\varepsilon_2\{2\}$ are shown in Fig. 2, where they are compared with available experimental data on $v_2\{4\}/v_2\{2\}$. The case $p = 1$, corresponding to wounded nucleon scaling, is in poor agreement with data. The ratio $\varepsilon_2\{4\}/\varepsilon_2\{2\}$ is below data, which means that the relative fluctuations of ε_2 are too large. In particular, $\varepsilon_2\{4\}$ falls too steeply for central collisions [29]. The other values $p = 0$ and $p = -1$, corresponding to saturation models, are in fair agreement with data.[2] Note that $\varepsilon_2\{4\}$ is essentially the mean eccentricity in the reaction plane in this centrality range [27]. Saturation-inspired models are known to predict a larger mean eccentricity in the reaction plane than the Glauber model [44, 45]. The larger mean eccentricity implies that relative fluctuations of ε_2 are smaller, therefore, the ratio $\varepsilon_2\{4\}/\varepsilon_2\{2\}$ is larger.

Above 20% centrality (not shown in figure), we find that all three models ($p = 1, 0, -1$) overpredict $v_2\{4\}/v_2\{2\}$, much as in Fig. 1 (a). Therefore, for mid-central and peripheral collisions, all parameterizations of initial conditions require a nonlinear hydrodynamic response, breaking Eq. (3), in order to be compatible with data.

[2] A comparison of the behaviors of $v_2\{2\}$ and $\varepsilon_2\{2\}$ in the 0-5% centrality range also shows that the MC-KLN model is in better agreement with data than the Glauber model [41].

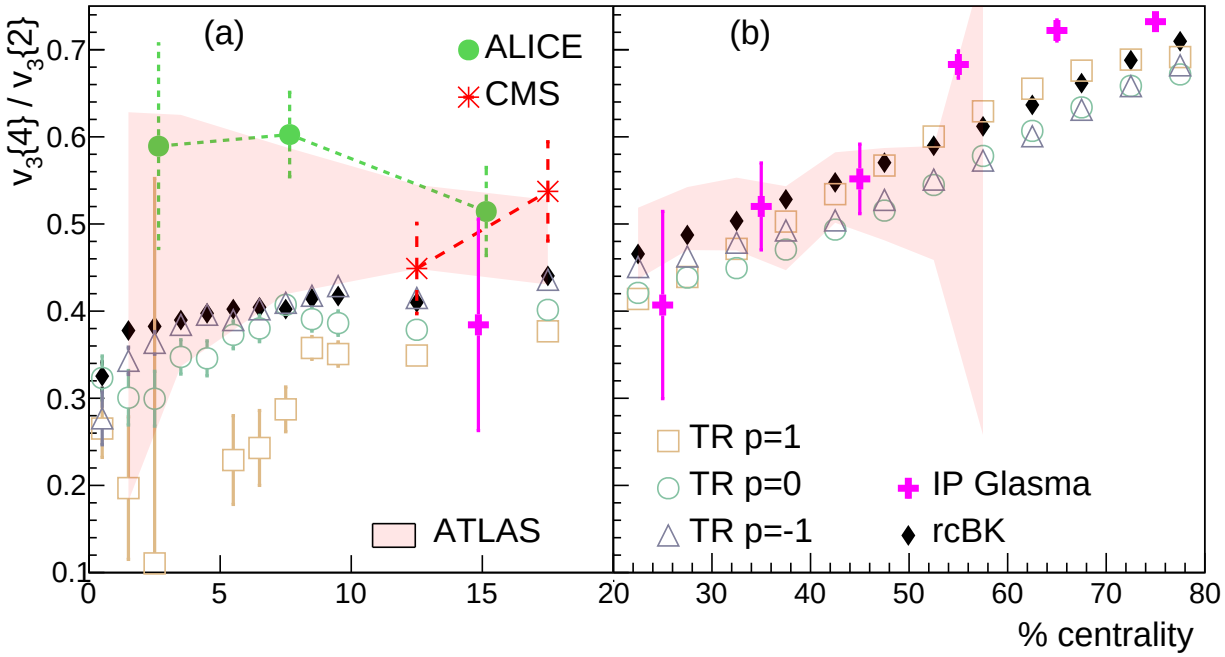

FIG. 3. (color online) Test of initial condition models using $v_3\{4\}/v_3\{2\}$ measured in 2.76 TeV Pb+Pb collisions: (a) up to 20% centrality; (b) between 20 and 80% centrality. Stars: CMS data [46]. Full circles: ALICE data [41]. Shaded band: ATLAS data [24]. ALICE and CMS data are not shown in panel (b) for the sake of readability, but are compatible with ATLAS data. Remaining symbols correspond to values of $\varepsilon_3\{4\}/\varepsilon_3\{2\}$ from several models of initial conditions. Open symbols: T$_\mathrm{R}$ENTo, with $p = -1$ (triangles), $p = 0$ (circles), $p = 1$ (squares). Full crosses: IP Glasma [18]. Full diamonds: Monte Carlo rcBK [16].

B. Triangular flow fluctuations

We now test the validity of Eq. (3) in the case of triangular flow fluctuations. Hydrodynamic results in Fig. 1 (b) show that, as in the case of elliptic flow, $\varepsilon_3\{4\}/\varepsilon_3\{2\}$ is systematically larger than $v_3\{4\}/v_3\{2\}$ above 40% centrality. This can again be attributed to a nonlinear hydrodynamic response, whose effect is however smaller for v_3 than for v_2. It could be due to a coupling between v_2 and v_1 [5]. In general, one expects any nonlinear response to be associated with the large magnitude of v_2, which is by far the largest Fourier harmonic [47]. One therefore expects nonlinear effects to be small for central collisions, even though the large error bars in our calculation prevent any definite conclusion.

Since nonlinear effects are smaller for v_3 than for v_2, we compare $v_3\{4\}/v_3\{2\}$ from data with $\varepsilon_3\{4\}/\varepsilon_3\{2\}$ from initial state models across the full centrality range. We use the same parameterizations of the T$_\mathrm{R}$ENTo model as in Fig. 2. We also implement two other initial-state models, IP-Glasma [18] and Monte Carlo rcBK [16]. Results are displayed in Fig. 3, where the 0-20% centrality range is zoomed in (panel (a)) for sake or readability. A first remark is that experimental data do not exhibit any clear dependence on centrality. Relative ε_3 fluctuations, on the other hand, grow from central to peripheral collisions for all models. This centrality dependence has a simple explanation: The system size decreases as a function of the centrality percentile, therefore relative ε_3 fluctuations become larger [48]. In general, the nonlinear hydrodynamic response seen in Fig. 1 (b) would help decreasing $v_3\{4\}/v_3\{2\}$ above 40% centrality, and reducing the centrality dependence which is seen in models and not in data. However, all configurations of T$_\mathrm{R}$ENTo in Fig. 3 (b) are compatible with ATLAS data above 40% centrality, and some points would fall below data if a nonlinear response was included.

Fig. 3 (a) presents results in the 20% most central collisions, where we use a finer centrality binning for initial-state models. In this centrality range, we do not foresee any significant nonlinear hydrodynamic response, and initial state calculations should match data. Data points (in particular from ALICE) are however above all models. As observed for elliptic flow, the wounded nucleon prescription (p=1) gives the worst results. All initial state models overestimate the relative fluctuations of ε_3 in central Pb+Pb collisions.

C. Predictions for $v_3\{6\}$

We now use Eq. (3) to make predictions for $v_3\{6\}$ in Pb+Pb collisions. The number of events in our hydrodynamic calculations is not large enough to test directly the validity of Eq. (3) for $v_3\{6\}/v_3\{4\}$. However, we have noted that the nonlinear hydrodynamic

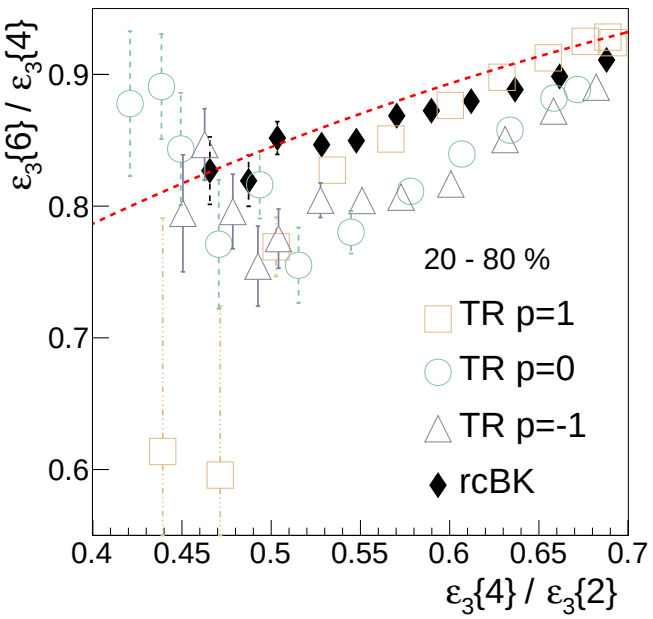

FIG. 4. (color online) Predictions for $v_3\{6\}/v_3\{4\}$ in 2.76 TeV Pb+Pb collisions, from several models of initial conditions, in the $20-80\%$ centrality range. Empty symbols: Predictions of T$_\mathrm{R}$ENTo with $p=1$ (squares), $p=0$ (circles), and $p=-1$ (triangles). Full diamonds: Prediction of Monte Carlo rcBK [16]. The red dashed line is the prediction of the Power distribution [49].

response is smaller for v_3 than for v_2. In addition, a previous study [27] has shown that even for v_2, the ratio $v_2\{6\}/v_2\{4\}$ is little affected by the nonlinear response, so that Eq. (3) applies to a good approximation. We therefore assume that Eq. (3) also gives a reasonable estimate of $v_3\{6\}/v_3\{4\}$, and we make predictions on this basis using the T$_\mathrm{R}$ENTo model and the rcBK model.

It has been argued that the probability distribution of ε_3 [50], which is solely due to fluctuations, is well described by the Power distribution [49], which has a single free parameter characterizing the rms value of ε_3. If the distribution of ε_3 follows the Power distribution, then the ratio $\varepsilon_3\{6\}/\varepsilon_3\{4\}$ is a simple function of the ratio $\varepsilon_3\{4\}/\varepsilon_3\{2\}$, which is displayed as a dashed line in Fig. 4. By running Monte Carlo simulations of the initial state, we can test whether the results fall on this line. We simulate a large number of Pb+Pb collisions in the $20-80\%$ centrality range.

Results are shown as symbols in Fig. 4. The centrality percentile corresponding to each symbol can be inferred from Fig. 3 (b). For a given model, $\varepsilon_3\{4\}/\varepsilon_3\{2\}$ increases with the centrality percentile. The rcBK model follows the prediction of the Power distribution, while the various parameterizations of the Trento model give in general smaller values of $\varepsilon_3\{6\}/\varepsilon_3\{4\}$. The fact that the Power distribution can be a poor approximation for large systems such as Pb+Pb collisions, even if the anisotropy is solely due to fluctuations, has already been pointed out in Ref. [51]. Even though precise figures depend on the particular model used, we predict on the basis of our Monte Carlo calculations and of Eq. (3) that $v_3\{6\}/v_3\{4\}$ should lie between 0.75 and 0.85 in the $30-50\%$ centrality range.

IV. HIGH-MULTIPLICITY p+Pb COLLISIONS

In this Section, we study relative flow fluctuations in high-multiplicity p+Pb collisions at $\sqrt{s}=5.02$ TeV and make quantitative predictions for higher-order cumulants of v_2 and v_3. Elliptic and triangular flow have been measured in this system [25, 52–54]. In particular, a positive $v_2\{4\}^4$ has been reported by all collaborations, which suggests that the measured azimuthal correlations originate from a collective effect. Hydrodynamic simulations have also been carried out [55–60] with IP-Glasma or Glauber initial conditions, and satisfactory agreement with data was found, which supports the hydrodynamic picture as a valid description of this system [61]. Since elliptic flow is significantly smaller in p+Pb collisions than in Pb+Pb collisions [62], one does not expect a significant nonlinear hydrodynamic response, and we assume that Eq. (3) always holds. Event-by-event hydrodynamic simulations confirm that v_2 and v_3 scale linearly with the corresponding initial anisotropies ε_2 and ε_3 [55].

We first select a model of initial conditions by requiring that it reproduces the first non trivial ratio $v_2\{4\}/v_2\{2\}$, which has been measured by the CMS Collaboration [53] as a function of centrality. As in the previous section, we use the T$_\mathrm{R}$ENTo model. However, the sets of parameters that give a reasonable description of Pb+Pb data fail to describe p+Pb data. Specifically, the values $p=-1$ and $p=0$, which work well in Fig. 2, yield a negative $\varepsilon_2\{4\}^4$ in p+Pb collisions (hence $\varepsilon_2\{4\}$ is undefined), and smaller values of ε_2 than needed to explain the observed v_2. This is due to the fact that with these parameters, the initial density profile is included in the transverse area spanned by the proton, which is circular. For the same reason, the IP-Glasma model underpredicts v_2 by a large factor unless one allows the proton to be "eccentric" [58]. On the other hand, previous hydrodynamic calculations have shown that Glauber initial conditions yield results in good agreement with p+Pb data. We therefore choose the value $p=1$ corresponding to the Glauber model, even though it does not give a good description of Pb+Pb data. We fix the parameter governing the multiplicity fluctuations to the value $k=0.9$ [55], and we have checked that the initial entropy distribution folded with a Poisson distribution yields the final multiplicity distribution observed in experiments [42]. We allow the width σ of the source associated with each nucleon to vary. The default value in previous calculations is $\sigma=0.4$ fm. As we shall see, results depend somewhat on the value of σ.

Figure 5 (a) displays the comparison between $\varepsilon_2\{4\}/\varepsilon_2\{2\}$ from the T$_\mathrm{R}$ENTo model and $v_2\{4\}/v_2\{2\}$

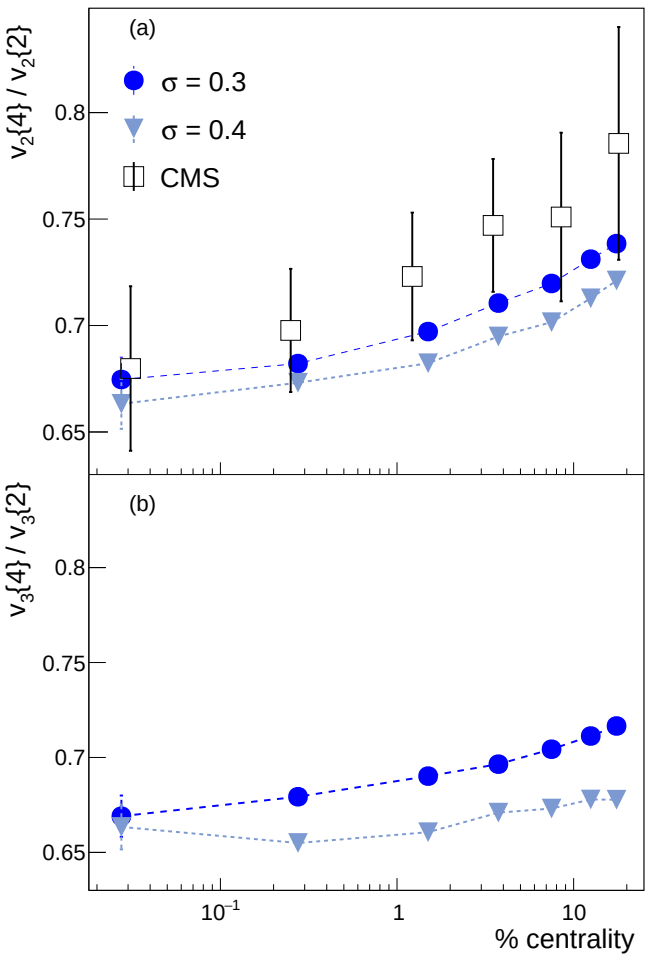

FIG. 5. (color online) $v_2\{4\}/v_2\{2\}$ (a) and $v_3\{4\}/v_3\{2\}$ (b) as functions of centrality percentile in 5.02 TeV p+Pb collisions. Full circles: TRENTo parametrization with $\sigma = 0.3$ fm. Triangles: TRENTo parametrization with $\sigma = 0.4$ fm. Squares: CMS data [53]. The centrality binning of CMS data is taken from Table I of Ref. [59].

measured by CMS [53]. The centrality percentile in the model is defined from the multiplicity of produced particles, thus mimicking the experimental situation. For $\sigma = 0.4$ fm, the model is compatible with experimental data in ultracentral collisions, but underestimates the ratio of cumulants when the centrality percentile increases. These results are consistent with the hydrodynamic results by Kozlov *et al.* [59], who find that $v_2\{2\}$ matches data but $v_2\{4\}$ is slightly too small. Agreement with experimental data slightly improves if the source width is lowered to $\sigma = 0.3$ fm. Lower values of σ yield more spiky initial density profiles, and are known to increase the magnitude of ε_2 and ε_3 in small systems [14]. Larger ε_n also implies larger $\varepsilon_n\{4\}/\varepsilon_n\{2\}$ [49]. Even with $\sigma = 0.3$ fm, our parameterization of initial conditions tends to underpredict $v_2\{4\}/v_2\{2\}$. Note, however, that the measurements of $v_2\{4\}$ and $v_2\{2\}$ differ in the implementation, and comparing them may not be apples to apples: $v_2\{2\}$ is measured with a large pseudorapidity gap to suppress nonflow effects, but there is no gap in $v_2\{4\}$. Therefore, $v_2\{4\}$ may have a sensitivity to nonflow short range (near side) correlations. In addition, the η gap typically reduces $v_2\{2\}$ because of pseudorapidity dependent event plane fluctuations [63]. Recently, a novel method to measure multi-particle cumulants in small systems has been proposed [64]. It implements pseudorapidity gaps for the measurements of four-particle correlations. The authors of this method show explicitly that nonflow contributions can account for almost 30% of the measured four-particle correlations ($v_2\{4\}$ and $v_3\{4\}$) in proton+proton collisions. We expect agreement between our model and experimental data to be improved if $v_2\{2\}$ and $v_2\{4\}$ are measured using the same particles.

We now make predictions for the ratio $v_3\{4\}/v_3\{2\}$, which is not yet measured in p+Pb collisions. $v_3\{4\}$ has been computed in event-by-event hydrodynamics [59]. The ratio $v_3\{4\}/v_3\{2\}$ is a more robust quantity, in the sense that depends little on model parameters (viscosity, freeze-out temperature) and kinematic cuts (p_t). Our results are shown in Fig. 5 (b). We predict that $v_3\{4\}/v_3\{2\}$ is close to $v_2\{4\}/v_2\{2\}$, but slightly smaller. The dependence on σ is somewhat stronger for v_3 than for v_2.

The CMS Collaboration has also measured $v_2\{6\}/v_2\{4\}$ and $v_2\{8\}/v_2\{6\}$ [25]. Our TRENTo results for these ratios are shown in Fig. 6. As in Fig. 4, we plot them as a function of the lowest order ratio $v_2\{4\}/v_2\{2\}$. Our Monte Carlo results are in perfect agreement with the prediction from the Power distribution. This confirms the prediction that the Power distribution should work well for small systems, irrespective of model details [51]. Existing CMS data are in good agreement with this theory prediction. Future measurements with smaller error bars will provide a crucial test that v_2 originates from the spatial eccentricity ε_2.

We finally make a prediction for $v_3\{6\}/v_3\{4\}$ as function of $v_3\{4\}/v_3\{2\}$ in central p+Pb collisions. Results are displayed in Fig. 7 for both $\sigma = 0.3$ fm and $\sigma = 0.4$ fm. Monte Carlo results are again reasonably well described by the Power distribution, with large error bars for $\sigma = 0.4$ fm.

V. DISCUSSION AND OUTLOOK

We have shown that ratios of cumulants are a powerful tool to test models of initial conditions. Elliptic flow data in central Pb+Pb collisions exclude the Glauber model, while saturation models (mimicked by the TRENTo parameterization with $p = 0$ or $p = -1$) are compatible with data. However, models which work for v_2 still overpredict the fluctuations of v_3 in central Pb+Pb collisions. A possible explanation is that these models overestimate both the fluctuations, and the mean eccentricity in the reaction plane, in such a way that the error cancels in

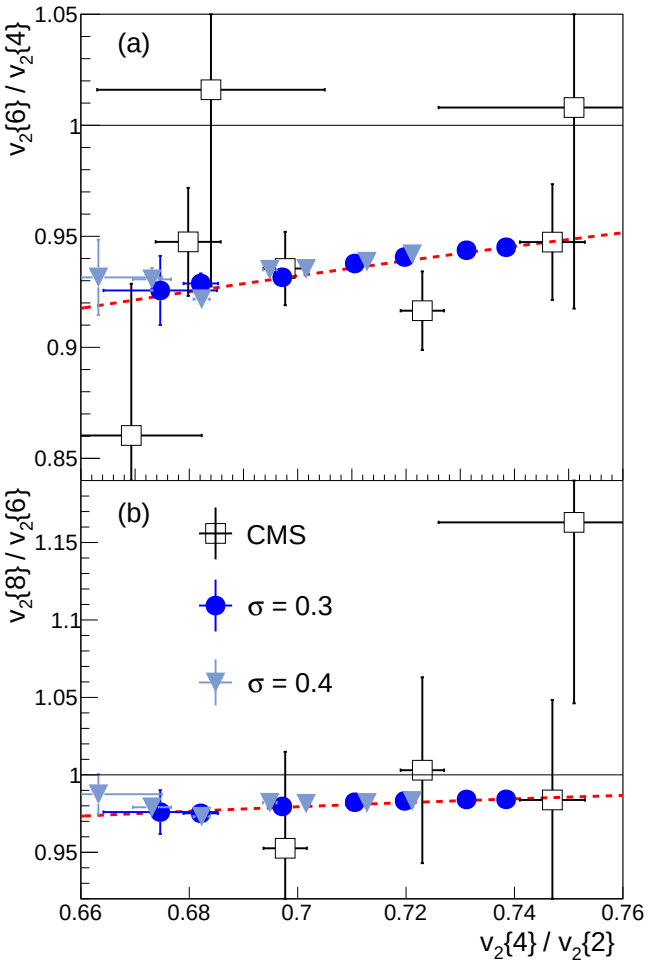

FIG. 6. (color online) Eccentricity-driven predictions for $v_2\{6\}/v_2\{4\}$ and $v_2\{8\}/v_2\{6\}$ as function of $v_2\{4\}/v_2\{2\}$ in 5.02 TeV p+Pb collisions. Full symbols: TRENTo parametrization with $\sigma = 0.3$ fm (circles) and $\sigma = 0.4$ fm (triangles). Empty symbols: CMS data [25]. The red dashed line represents the prediction of the Power distribution [49].

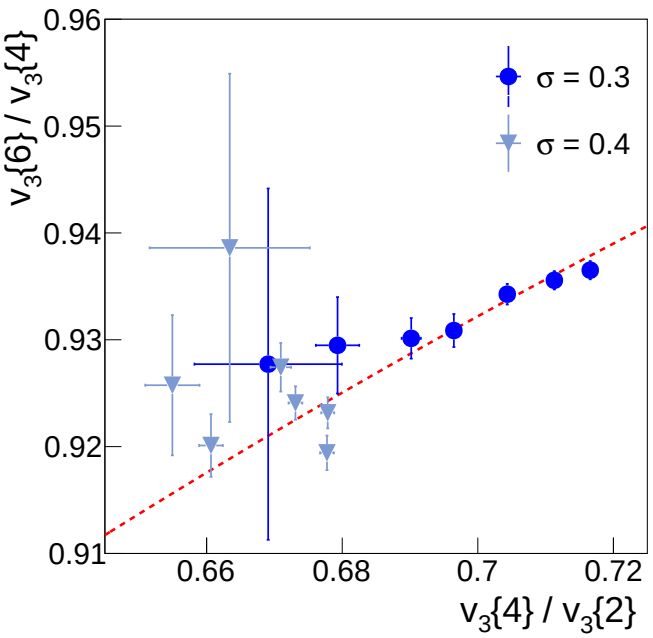

FIG. 7. (color online) Prediction for $v_3\{6\}/v_3\{4\}$ as function of $v_3\{4\}/v_3\{2\}$ in central 5.02 TeV p+Pb collisions, from different TRENTo parametrizations. Circles: $\sigma = 0.3$ fm. Triangles: $\sigma = 0.4$ fm. The red dashed line represents the prediction of the Power distribution [49].

the ratio for v_2, but not for v_3 which is solely due to fluctuations. It will be of crucial importance to reduce the error bars for $v_3\{4\}$ in central Pb+Pb collisions, in order to check whether the ratio $v_3\{4\}/v_3\{2\}$ is independent of centrality, as suggested by ALICE data: Indeed, this observation does not seem compatible with existing models of initial conditions.

The parameterizations of the initial state which work for Pb+Pb collisions do not work for p+Pb collisions and vice versa. The Glauber model, which is excluded by Pb+Pb data, works well for p+Pb collisions. We do not consider this a contradiction, since we are merely trying to identify the parameterization which captures the initial geometry in a given system, and do not aim at a unified description of all systems. We predict that the ratio $v_3\{4\}/v_3\{2\}$ is very close to $v_2\{4\}/v_2\{2\}$ in high-multiplicity p+Pb collisions. However, nonflow effects differ for v_2 and v_3 (back to back correlations typically increase v_2 and decrease v_3) and must be carefully removed in the analysis.

Our analysis could eventually be extended to high-multiplicity proton-proton collisions, where observed azimuthal multi-particle correlations suggest that collective effects are also present [26, 65]. These new data have triggered new models of initial conditions [13, 66]. These new models can be tested against data using ratios of cumulants, much in the same way as for p+Pb collisions.

ACKNOWLEDGEMENTS

JNH acknowledges the use of the Maxwell Cluster and the advanced support from the Center of Advanced Computing and Data Systems at the University of Houston and was supported by the National Science Foundation under grant no. PHY-1513864. We thank Matt Luzum for useful discussions. GG wishes to thank Scott Moreland for kind assistance with the use of TRENTo.

Appendix A: The TRENTo model

The TRENTo model is a flexible parametric Monte Carlo model for the initial conditions of heavy-ion collisions, which encompasses several other models [42]. Consider the case of a nucleon A colliding with a nucleon B. Each participant nucleon deposits entropy in the transverse plane according to a Gaussian distribution of width

σ, which reads

$$S_{A,B} = w_{\mathrm{A,B}}\ \frac{1}{2\pi\sigma^2}\exp\left[\frac{(x-x_{\mathrm{A,B}})^2+(y-y_{\mathrm{A,B}})^2}{2\sigma^2}\right]. \tag{A1}$$

The normalization w is a random number which is assigned to each participant nucleon. Its probability distribution is a Γ distribution whose mean value is equal to unity, and width is regulated by a parameter k. The initial entropy profile is computed through a generalized average of thickness functions, which reads

$$S(p; S_{\mathrm{A}}, S_{\mathrm{B}}) = \left(\frac{S_{\mathrm{A}}^p + S_{\mathrm{B}}^p}{2}\right)^{\frac{1}{p}}, \tag{A2}$$

where p is an arbitrary real parameter. The previous formula can be generalized to the case of a nucleus A colliding with a nucleus B [42]. Note that for $p = 1$ nuclear density profiles are superimposed ($S \propto S_{\mathrm{A}} + S_{\mathrm{B}}$). If $p = 0$, or $p = -1$, instead, the initial entropy deposition is computed through the product of the two nuclear density profiles ($S \propto S_{\mathrm{A}} S_{\mathrm{B}}$). Varying the value of p, it is possible to construct initial entropy profiles according to different prescriptions [43]: $p = 1$ is the wounded nucleon model; lower values of p reproduce QCD-based models, such as EKRT [67] ($p = 0$), or Monte Carlo KLN [68] ($p = -0.67$).

[1] M. Luzum, J. Phys. G **38**, 124026 (2011) doi:10.1088/0954-3899/38/12/124026 [arXiv:1107.0592 [nucl-th]].

[2] D. Teaney and L. Yan, Phys. Rev. C **83**, 064904 (2011) doi:10.1103/PhysRevC.83.064904 [arXiv:1010.1876 [nucl-th]].

[3] F. G. Gardim, F. Grassi, M. Luzum and J. Y. Ollitrault, Phys. Rev. C **85**, 024908 (2012) doi:10.1103/PhysRevC.85.024908 [arXiv:1111.6538 [nucl-th]].

[4] H. Niemi, G. S. Denicol, H. Holopainen and P. Huovinen, Phys. Rev. C **87**, no. 5, 054901 (2013) doi:10.1103/PhysRevC.87.054901 [arXiv:1212.1008 [nucl-th]].

[5] F. G. Gardim, J. Noronha-Hostler, M. Luzum and F. Grassi, Phys. Rev. C **91**, no. 3, 034902 (2015) doi:10.1103/PhysRevC.91.034902 [arXiv:1411.2574 [nucl-th]].

[6] B. Alver *et al.* [PHOBOS Collaboration], Phys. Rev. Lett. **98**, 242302 (2007) doi:10.1103/PhysRevLett.98.242302 [nucl-ex/0610037].

[7] G. Aad *et al.* [ATLAS Collaboration], JHEP **1311**, 183 (2013) doi:10.1007/JHEP11(2013)183 [arXiv:1305.2942 [hep-ex]].

[8] T. Renk and H. Niemi, Phys. Rev. C **89**, no. 6, 064907 (2014) doi:10.1103/PhysRevC.89.064907 [arXiv:1401.2069 [nucl-th]].

[9] L. Yan, J. Y. Ollitrault and A. M. Poskanzer, Phys. Lett. B **742**, 290 (2015) doi:10.1016/j.physletb.2015.01.039 [arXiv:1408.0921 [nucl-th]].

[10] M. L. Miller, K. Reygers, S. J. Sanders and P. Steinberg, Ann. Rev. Nucl. Part. Sci. **57**, 205 (2007) doi:10.1146/annurev.nucl.57.090506.123020 [nucl-ex/0701025].

[11] M. Alvioli, H.-J. Drescher and M. Strikman, Phys. Lett. B **680**, 225 (2009) doi:10.1016/j.physletb.2009.08.067 [arXiv:0905.2670 [nucl-th]].

[12] M. Rybczynski, G. Stefanek, W. Broniowski and P. Bozek, Comput. Phys. Commun. **185**, 1759 (2014) doi:10.1016/j.cpc.2014.02.016 [arXiv:1310.5475 [nucl-th]].

[13] C. Loizides, Phys. Rev. C **94**, no. 2, 024914 (2016) doi:10.1103/PhysRevC.94.024914 [arXiv:1603.07375 [nucl-ex]].

[14] B. G. Zakharov, arXiv:1611.05825 [nucl-th].

[15] H.-J. Drescher and Y. Nara, Phys. Rev. C **75**, 034905 (2007) doi:10.1103/PhysRevC.75.034905 [nucl-th/0611017].

[16] J. L. ALbacete and A. Dumitru, arXiv:1011.5161 [hep-ph].

[17] K. Werner, I. Karpenko, T. Pierog, M. Bleicher and K. Mikhailov, Phys. Rev. C **82**, 044904 (2010) doi:10.1103/PhysRevC.82.044904 [arXiv:1004.0805 [nucl-th]].

[18] B. Schenke, P. Tribedy and R. Venugopalan, Phys. Rev. Lett. **108**, 252301 (2012) doi:10.1103/PhysRevLett.108.252301 [arXiv:1202.6646 [nucl-th]].

[19] J. L. Albacete and C. Marquet, Prog. Part. Nucl. Phys. **76**, 1 (2014) doi:10.1016/j.ppnp.2014.01.004 [arXiv:1401.4866 [hep-ph]].

[20] H. Niemi, K. J. Eskola and R. Paatelainen, Phys. Rev. C **93**, no. 2, 024907 (2016) doi:10.1103/PhysRevC.93.024907 [arXiv:1505.02677 [hep-ph]].

[21] N. Borghini, P. M. Dinh and J. Y. Ollitrault, Phys. Rev. C **64**, 054901 (2001) doi:10.1103/PhysRevC.64.054901 [nucl-th/0105040].

[22] A. Bilandzic, R. Snellings and S. Voloshin, Phys. Rev. C **83**, 044913 (2011) doi:10.1103/PhysRevC.83.044913 [arXiv:1010.0233 [nucl-ex]].

[23] P. Di Francesco, M. Guilbaud, M. Luzum and J. Y. Ollitrault, arXiv:1612.05634 [nucl-th].

[24] G. Aad *et al.* [ATLAS Collaboration], Eur. Phys. J. C **74**, no. 11, 3157 (2014) doi:10.1140/epjc/s10052-014-3157-z [arXiv:1408.4342 [hep-ex]].

[25] V. Khachatryan *et al.* [CMS Collaboration], Phys. Rev. Lett. **115**, no. 1, 012301 (2015) doi:10.1103/PhysRevLett.115.012301 [arXiv:1502.05382 [nucl-ex]].

[26] V. Khachatryan *et al.* [CMS Collaboration], Phys. Lett. B **765**, 193 (2017) doi:10.1016/j.physletb.2016.12.009 [arXiv:1606.06198 [nucl-ex]].

[27] G. Giacalone, L. Yan, J. Noronha-Hostler and J. Y. Ollitrault, Phys. Rev. C **95**, no. 1, 014913 (2017) doi:10.1103/PhysRevC.95.014913 [arXiv:1608.01823 [nucl-th]].

[28] L. Ma, G. L. Ma and Y. G. Ma, Phys. Rev. C **94**, no. 4, 044915 (2016) doi:10.1103/PhysRevC.94.044915 [arXiv:1610.04733 [nucl-th]].

[29] R. S. Bhalerao, M. Luzum and J. Y. Ollitrault, Phys. Rev. C **84**, 034910 (2011) doi:10.1103/PhysRevC.84.034910 [arXiv:1104.4740 [nucl-th]].

[30] S. A. Voloshin, A. M. Poskanzer, A. Tang and G. Wang, Phys. Lett. B **659**, 537 (2008) doi:10.1016/j.physletb.2007.11.043 [arXiv:0708.0800 [nucl-th]].

[31] E. Retinskaya, M. Luzum and J. Y. Ollitrault, Phys. Rev. C **89**, no. 1, 014902 (2014) doi:10.1103/PhysRevC.89.014902 [arXiv:1311.5339 [nucl-th]].

[32] C. Loizides, J. Nagle and P. Steinberg, SoftwareX **1-2**, 13 (2015) doi:10.1016/j.softx.2015.05.001 [arXiv:1408.2549 [nucl-ex]].

[33] J. Noronha-Hostler, G. S. Denicol, J. Noronha, R. P. G. Andrade and F. Grassi, Phys. Rev. C **88**, no. 4, 044916 (2013) doi:10.1103/PhysRevC.88.044916 [arXiv:1305.1981 [nucl-th]].

[34] J. Noronha-Hostler, J. Noronha and F. Grassi, Phys. Rev. C **90**, no. 3, 034907 (2014) doi:10.1103/PhysRevC.90.034907 [arXiv:1406.3333 [nucl-th]].

[35] J. Noronha-Hostler, J. Noronha and M. Gyulassy, Phys. Rev. C **93**, no. 2, 024909 (2016) doi:10.1103/PhysRevC.93.024909 [arXiv:1508.02455 [nucl-th]].

[36] G. Policastro, D. T. Son and A. O. Starinets, Phys. Rev. Lett. **87**, 081601 (2001) doi:10.1103/PhysRevLett.87.081601 [hep-th/0104066].

[37] D. Teaney, Phys. Rev. C **68**, 034913 (2003) doi:10.1103/PhysRevC.68.034913 [nucl-th/0301099].

[38] B. Alver and G. Roland, Phys. Rev. C **81**, 054905 (2010) Erratum: [Phys. Rev. C **82**, 039903 (2010)] doi:10.1103/PhysRevC.82.039903, 10.1103/PhysRevC.81.054905 [arXiv:1003.0194 [nucl-th]].

[39] J. Noronha-Hostler, L. Yan, F. G. Gardim and J. Y. Ollitrault, Phys. Rev. C **93**, no. 1, 014909 (2016) doi:10.1103/PhysRevC.93.014909 [arXiv:1511.03896 [nucl-th]].

[40] S. Chatrchyan *et al.* [CMS Collaboration], Phys. Rev. C **87**, no. 1, 014902 (2013) doi:10.1103/PhysRevC.87.014902 [arXiv:1204.1409 [nucl-ex]].

[41] K. Aamodt *et al.* [ALICE Collaboration], Phys. Rev. Lett. **107**, 032301 (2011) doi:10.1103/PhysRevLett.107.032301 [arXiv:1105.3865 [nucl-ex]].

[42] J. S. Moreland, J. E. Bernhard and S. A. Bass, Phys. Rev. C **92**, no. 1, 011901 (2015) doi:10.1103/PhysRevC.92.011901 [arXiv:1412.4708 [nucl-th]].

[43] J. E. Bernhard, J. S. Moreland, S. A. Bass, J. Liu and U. Heinz, Phys. Rev. C **94**, no. 2, 024907 (2016) doi:10.1103/PhysRevC.94.024907 [arXiv:1605.03954 [nucl-th]].

[44] T. Hirano, U. W. Heinz, D. Kharzeev, R. Lacey and Y. Nara, Phys. Lett. B **636**, 299 (2006) doi:10.1016/j.physletb.2006.03.060 [nucl-th/0511046].

[45] T. Lappi and R. Venugopalan, Phys. Rev. C **74**, 054905 (2006) doi:10.1103/PhysRevC.74.054905 [nucl-th/0609021].

[46] S. Chatrchyan *et al.* [CMS Collaboration], Phys. Rev. C **89**, no. 4, 044906 (2014) doi:10.1103/PhysRevC.89.044906 [arXiv:1310.8651 [nucl-ex]].

[47] D. Teaney and L. Yan, Phys. Rev. C **86**, 044908 (2012) doi:10.1103/PhysRevC.86.044908 [arXiv:1206.1905 [nucl-th]].

[48] R. S. Bhalerao, M. Luzum and J. Y. Ollitrault, Phys. Rev. C **84**, 054901 (2011) doi:10.1103/PhysRevC.84.054901 [arXiv:1107.5485 [nucl-th]].

[49] L. Yan and J. Y. Ollitrault, Phys. Rev. Lett. **112**, 082301 (2014) doi:10.1103/PhysRevLett.112.082301 [arXiv:1312.6555 [nucl-th]].

[50] L. V. Bravina *et al.*, Eur. Phys. J. C **75**, no. 12, 588 (2015) doi:10.1140/epjc/s10052-015-3815-9 [arXiv:1509.02692 [hep-ph]].

[51] H. Grnqvist, J. P. Blaizot and J. Y. Ollitrault, Phys. Rev. C **94**, no. 3, 034905 (2016) doi:10.1103/PhysRevC.94.034905 [arXiv:1604.07230 [nucl-th]].

[52] G. Aad *et al.* [ATLAS Collaboration], Phys. Lett. B **725**, 60 (2013) doi:10.1016/j.physletb.2013.06.057 [arXiv:1303.2084 [hep-ex]].

[53] S. Chatrchyan *et al.* [CMS Collaboration], Phys. Lett. B **724**, 213 (2013) doi:10.1016/j.physletb.2013.06.028 [arXiv:1305.0609 [nucl-ex]].

[54] B. B. Abelev *et al.* [ALICE Collaboration], Phys. Rev. C **90**, no. 5, 054901 (2014) doi:10.1103/PhysRevC.90.054901 [arXiv:1406.2474 [nucl-ex]].

[55] P. Bozek and W. Broniowski, Phys. Rev. C **88**, no. 1, 014903 (2013) doi:10.1103/PhysRevC.88.014903 [arXiv:1304.3044 [nucl-th]].

[56] A. Bzdak, B. Schenke, P. Tribedy and R. Venugopalan, Phys. Rev. C **87**, no. 6, 064906 (2013) doi:10.1103/PhysRevC.87.064906 [arXiv:1304.3403 [nucl-th]].

[57] G. Y. Qin and B. Mller, Phys. Rev. C **89**, no. 4, 044902 (2014) doi:10.1103/PhysRevC.89.044902 [arXiv:1306.3439 [nucl-th]].

[58] B. Schenke and R. Venugopalan, Phys. Rev. Lett. **113**, 102301 (2014) doi:10.1103/PhysRevLett.113.102301 [arXiv:1405.3605 [nucl-th]].

[59] I. Kozlov, M. Luzum, G. Denicol, S. Jeon and C. Gale, arXiv:1405.3976 [nucl-th].

[60] C. Shen, J. F. Paquet, G. S. Denicol, S. Jeon and C. Gale, Phys. Rev. C **95**, no. 1, 014906 (2017) doi:10.1103/PhysRevC.95.014906 [arXiv:1609.02590 [nucl-th]].

[61] R. D. Weller and P. Romatschke, arXiv:1701.07145 [nucl-th].

[62] B. Abelev *et al.* [ALICE Collaboration], Phys. Lett. B **719**, 29 (2013) doi:10.1016/j.physletb.2013.01.012 [arXiv:1212.2001 [nucl-ex]].

[63] V. Khachatryan *et al.* [CMS Collaboration], Phys. Rev. C **92**, no. 3, 034911 (2015) doi:10.1103/PhysRevC.92.034911 [arXiv:1503.01692 [nucl-ex]].

[64] J. Jia, M. Zhou and A. Trzupek, arXiv:1701.03830 [nucl-th].

[65] G. Aad *et al.* [ATLAS Collaboration], Phys. Rev. Lett. **116**, no. 17, 172301 (2016) doi:10.1103/PhysRevLett.116.172301 [arXiv:1509.04776 [hep-ex]].

[66] K. Welsh, J. Singer and U. W. Heinz, Phys. Rev. C **94**, no. 2, 024919 (2016) doi:10.1103/PhysRevC.94.024919 [arXiv:1605.09418 [nucl-th]].

[67] K. J. Eskola, P. V. Ruuskanen, S. S. Rasanen and K. Tuominen, Nucl. Phys. A **696**, 715 (2001) doi:10.1016/S0375-9474(01)01207-6 [hep-ph/0104010].

[68] D. Kharzeev, E. Levin and M. Nardi, Nucl. Phys. A **747**, 609 (2005) doi:10.1016/j.nuclphysa.2004.10.018 [hep-ph/0408050].